

Dissipation-accelerated entanglement generation

Xiao-Wei Zheng¹, Jun-Cong Zheng¹, Xue-Feng Pan¹, Li-Hua Lin^{2,*}, Pei-Rong Han^{2,3}, and Peng-Bo Li^{1†}

¹*School of Physics, Xi'an Jiaotong University, Xi'an 710049, China*

²*Department of Physics,*

Fuzhou University, Fuzhou 350108, China

³*School of Physics and Mechanical and Electrical Engineering, Longyan University, Longyan, Fujian 364012, China*

(Dated: October 7, 2024)

Dissipation is usually considered a negative factor for observing quantum effects and for harnessing them for quantum technologies. Here we propose a scheme for speeding up the generation of quantum entanglement between two coupled qubits by introducing a strong dissipation channel to one of these qubits. The maximal entanglement is conditionally established by evenly distributing a single excitation between these two qubits. When the excitation is initially held by the dissipative qubit, the dissipation accelerates the excitation re-distribution process for the quantum state trajectory without quantum jumps. Our results show that the time needed to conditionally attain the maximal entanglement is monotonously decreased as the dissipative rate is increased. We further show that this scheme can be generalized to accelerate the production of the W state for the three-qubit system, where one NH qubit is symmetrically coupled to two Hermitian qubits.

INTRODUCTION

One of the most fundamental postulations of quantum mechanics is that the state of an isolated quantum system is described by a wavefunction, whose evolution is governed by a Hermitian Hamiltonian according to the Schrödinger equation. However, any quantum system is inevitably coupled to its surrounding environment, which acts as a meter that continuously acquires information about the system [1]. At the zero temperature, the environment can be regarded as a reservoir, composed of infinitely many bosonic modes, each initially in its vacuum state [2-4]. The system's information is gradually leaked into the reservoir by exchanging energy quanta. The most remarkable feature of this process is that the system's state evolution trajectory is significantly modified even if no quanta are leaked into the environment, as a consequence of measurement backaction.

For the no-jump trajectory, the system's evolution still can be described by the Schrödinger equation with a non-Hermitian (NH) Hamiltonian, featuring the competition between Hermitian and dissipative terms [5]. Such environment-induced non-Hermiticity endows the Hamiltonian's eigenstates and eigenenergies with striking features that are otherwise inaccessible, such as real-to-complex spectral phase transitions and NH topology [6-9]. So far, these NH effects have been experimentally demonstrated in distinct physical systems [10-30]. Recently, exceptional entanglement phenomena have been investigated in both theory and experiment in a NH spin-boson system [31]. In a very recent work [32], it was demonstrated that the entanglement between two interacting NH qubits can be generated within a time significantly shorter than that for two Hermitian ones. In the scheme, the two-qubit entanglement appears as a conse-

quence of the competition between the intra-qubit coupling and individual driving of the qubits, and the entanglement speedup is enabled by proximity to a higher-order exceptional point. Each NH qubit is realized with a three-level natural or artificial atom, where the highest and intermediate levels are used to encode the quantum information, and the non-Hermiticity is manifested by the decay from the intermediate to the lowest levels. This scheme is valid only when the decaying channel from the highest to intermediate levels is neglected. However, such a condition cannot be satisfied for general systems. For example, the decaying rate of the levels of a normal transmon linearly scales with the quantum number.

We here propose an alternative scheme for exploiting non-Hermiticity to speed up entanglement generation speedup between two qubits. The theoretical model involves a Hermitian qubit interacting with a decaying one by swapping coupling, which conserves the total excitation number. The entanglement is generated in the single-excitation subspace. The excitation, initially possessed by the NH qubit, is distributed between the two qubits by energy exchange. The maximal entanglement is attained when the two qubits are equally populated. We find that the non-Hermiticity significantly accelerates this excitation distribution process in a broad regime, enabling the two qubits to be entangled within a time much shorter than the dynamical timescale of the inter-qubit interaction. In distinct contrast with the scheme of Ref. [32], our approach does not require to encode the qubits in the highest and intermediate levels of a three-level system; the non-Hermiticity is manifested by the decay from the higher to lower levels of a two-level system. Furthermore, our scheme does not require individual driving of the qubits. Due to these simplifications, our scheme is not subjected to the errors coming from the decay of the

third level and from the fluctuations of individual drives, which are inherent in the previous scheme [33]. The idea can be directly extended to the three-qubit system, where a NH qubit is symmetrically coupled to two Hermitian ones. The dissipation of the NH qubit helps to speed up the generation of the three-qubit W-type maximally entangled state in a probabilistic manner.

TWO-QUBIT ENTANGLEMENT SPEEDUP

We here consider the system involving two qubits with the same frequency interacting with each other by swapping coupling, as shown in Fig. 1a. The non-Hermiticity of the system is manifested by the non-negligible dissipative rate of the first qubit, denoted as κ . The decaying rate of the second qubit is much smaller than the inter-qubit swapping rate λ , thereby negligible. The system dynamics is described by the master equation

$$\frac{d\hat{\rho}}{dt} = -i[\hat{\mathcal{H}}_{NH}, \rho] + \kappa \hat{\sigma}_1^- \rho \hat{\sigma}_1^+, \quad (1)$$

where $\hat{\mathcal{H}}_{NH}$ represents the two-qubit NH Hamiltonian, defined as

$$\hat{\mathcal{H}}_{NH} = \lambda(\hat{\sigma}_1^+ \hat{\sigma}_2^- + \hat{\sigma}_1^- \hat{\sigma}_2^+) - i\frac{\kappa}{2} |1\rangle_1 \langle 1|. \quad (2)$$

Here $\hat{\sigma}_j^+ = |1\rangle_j \langle 0|$ and $\hat{\sigma}_j^- = |0\rangle_j \langle 1|$ with $|1\rangle_j$ ($|0\rangle_j$) denoting the upper (lower) level of the j th qubit, and λ is inter-qubit coupling strength. The system evolution is a weighted mixture of infinitely many trajectories governed by the NH Hermitian but interrupted by randomly-occurring quantum jumps. For the trajectory without quantum jump, the system state evolution is governed by $\hat{\mathcal{H}}_{NH}$.

Under the NH Hamiltonian, the total excitation number of the qubits is conserved. Consequently, the qubit Hilbert space can be divided into three uncoupled subspaces $\mathcal{S}_0 = \{|0_1, 0_2\rangle\}$, $\mathcal{S}_1 = \{|1, 0\rangle, |0, 1\rangle\}$, and $\mathcal{S}_2 = \{|1, 1\rangle\}$. In \mathcal{S}_1 , the system has a pair of eigenenergies, given by

$$E_{\pm} = -i\kappa/4 \pm \Omega. \quad (3)$$

where $\Omega = \sqrt{\lambda^2 - \kappa^2/16}$. The corresponding eigenstates are

$$|\Phi_{\pm}\rangle = \mathcal{N}_{\pm}(E_{\pm} |1_1, 0_2\rangle + \lambda |0_1, 1_2\rangle), \quad (4)$$

where $\mathcal{N}_{\pm} = (|E_{\pm}|^2 + \lambda^2)^{-1/2}$. Suppose that the system is initially in the state $|\psi(0)\rangle = |1_1, 0_2\rangle$. Then the quantum state evolution associated with the no-jump trajectory can be rewritten as

$$|\psi(t)\rangle = \mathcal{N}(\mathcal{A} |1, 0\rangle - i\mathcal{B} |0, 1\rangle), \quad (5)$$

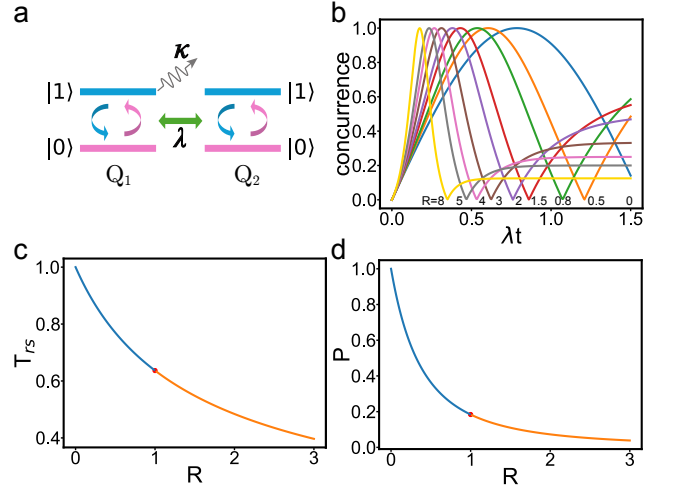


FIG. 1. (a) Sketch of the two-qubit system. The NH qubit (Q_1) and Hermitian qubit (Q_2) is resonantly coupled to each other with the strength λ . The upper level of Q_1 , $|1\rangle_1$, has a non-negligible decaying rate κ . (b) Two-qubit concurrences as functions of λt for different values of $R = \kappa/4\lambda$. The system evolves with the initial state $|1, 0\rangle$ under the NH Hamiltonian of Eq. (1). (c) Rescaled entangling time T_{rs} versus the rescaled dissipation rate R . Here T_{rs} is defined as the ratio between the times needed to reach maximal entanglement under the NH and Hermitian Hamiltonians with the same inter-qubit coupling λ . The dot denotes the exceptional point $R = 1$, where the entanglement time cannot be well defined. (d) Success probability for obtaining the maximally entangled state as a function of R . In the numerical simulations of (b), (c), and (d), the system evolves from the initial state $|1, 0\rangle$ under the NH Hamiltonian of Eq. (1).

where $\mathcal{N} = (\mathcal{A}^2 + \mathcal{B}^2)^{-1/2}$. When $R = \kappa/(4\lambda) < 1$, the coefficients \mathcal{A} and \mathcal{B} are given by

$$\begin{aligned} \mathcal{A} &= \cos(\Omega t) - \frac{\kappa}{4\Omega} \sin(\Omega t), \\ \mathcal{B} &= \frac{\lambda}{\Omega} \sin(\Omega t). \end{aligned}$$

For $R > 1$, the trigonometric functions are replaced by the corresponding hyperbolic functions, with $\Omega = \sqrt{\kappa^2/16 - \lambda^2}$. The two-qubit entanglement is quantified by the concurrence, given by [33]

$$\mathcal{E} = 2\mathcal{N}^2 \mathcal{A}\mathcal{B}. \quad (6)$$

To quantify to what extent the entanglement generation is speeded up by the non-Hermiticity, we define the rescaled entangling time, $T_{rs} = T/\tau$, where T is the shortest time needed to conditionally produce the two-qubit maximally entangled state for the NH system, and $\tau = \pi/4\lambda$ is the corresponding time for the Hermitian system. For $R < 1$, the rescaled entangling time is given by

$$T_{rs} = \frac{4}{\pi} \frac{1}{\sqrt{1-R^2}} \arctan \sqrt{\frac{1-R}{1+R}}. \quad (7)$$

When $R > 1$, T_{rs} is

$$T_{rs} = \frac{4}{\pi} \frac{1}{\sqrt{R^2 - 1}} \text{arc tanh} \sqrt{\frac{R-1}{R+1}}, \quad (8)$$

To quantitatively confirm the non-Hermiticity-enabled entanglement speedup, in Fig. 1b we present the two-qubit concurrence, associated with the no-jump trajectory, as a function of λt and R . The result clearly shows that the concurrence \mathcal{E} exhibits a non-monotonous behavior, and can reach the maximum 1 no matter when $R < 1$ or $R > 1$. The time needed to reach the maximal entanglement ($\mathcal{E} = 1$) is monotonously decreased with the increase of κ . When $R > 1$, after reaching the maximum \mathcal{E} drops to zero at the time $t = G^{-1} \text{arc tanh}(4G/\kappa)$, and then monotonously tends towards $\mathcal{E}_{t \rightarrow \infty} = 2x/(1+x^2)$, where $x = (G-\kappa/4)/\lambda$. For $R \gg 1$, $\mathcal{E}_{t \rightarrow \infty} \simeq 1/(2R)$. Fig. 1c display the rescaled entangling time T_{sc} versus the ratio R . The results clearly show that the entanglement generation is indeed speeded up by the non-Hermiticity, and T_{sc}^{2q} has a maximum 1 when $\kappa = 0$. The result can be interpreted as follows. The maximal entanglement is reached when the populations of $|1, 0\rangle$ and $|0, 1\rangle$, $P_{1,0}$ and $P_{0,1}$, are balanced. For the unitary evolution, this is achieved by coherent excitation transfer. When the excitation is initially populated in the NH qubit, the leakage of its population from the NH qubit to the environment help to increase the ratio $P_{0,1}/P_{1,0}$ from 0 to 1.

This entanglement dynamics is in stark contrast with that presented in Re. [32], where the system starts with the initial state $|0, 1\rangle$. For such an initial state, the system evolution associated with the no-jump trajectory is given by [32]

$$|\psi'(t)\rangle = \mathcal{N}'(\mathcal{A}'|0, 1\rangle - i\mathcal{B}'|1, 0\rangle), \quad (9)$$

where $\mathcal{A}' = \cos(\Omega t) + \frac{\kappa}{4\Omega} \sin(\Omega t)$ and $\cosh(Gt) + \frac{\kappa}{4G} \sinh(Gt)$ for $R < 1$ and $R > 1$, respectively. The two-qubit entanglement is $\mathcal{E}' = 2\mathcal{N}'^2 \mathcal{A}'\mathcal{B}'$. For $R < 1$, the rescaled entangling time is

$$T'_{rs} = \frac{4}{\pi} \frac{1}{\sqrt{1-R^2}} \arctan \sqrt{\frac{1+R}{1-R}}. \quad (10)$$

Contrary to the case with the initial state $|1, 0\rangle$, T'_{rs} increases with R . This is due to the fact that the dissipation plays a negative role in the transfer of the excitation from the Hermitian qubit to the NH qubit, so that it takes a longer time to balance $P_{1,0}$ and $P_{0,1}$. When $R > 1$, \mathcal{E} is monotonously increased, tending to a fixed value, which is smaller than 1 and is decreased when R increases. The results imply that the dissipation can speed up entanglement only when excitation is initially held by the NH qubit.

It is worthwhile to investigate to what extent the success probability of producing the maximally entangled

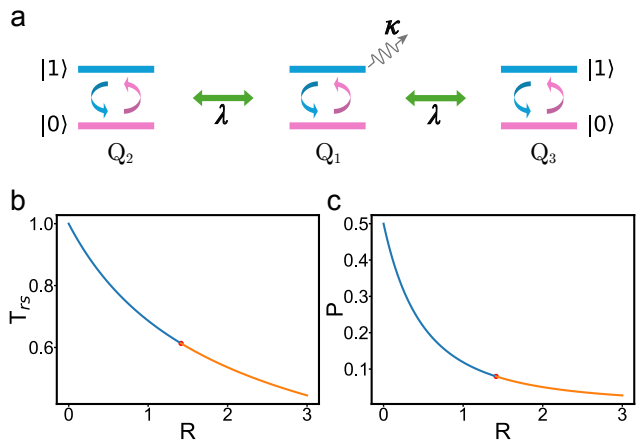


FIG. 2. (a) Sketch of the three-qubit system. One NH qubit (Q_1) is symmetrically coupled to two Hermitian qubits, Q_2 and Q_3 , with the strength λ . (b) Rescaled entangling time T_{rs} versus the R . Here T_{rs} is defined as the ratio between the times needed to reach the W-type maximally entangled state under the NH and Hermitian Hamiltonians with the same inter-qubit coupling λ . The system is initially in the state $|1, 0, 0\rangle$ and evolves under the three-qubit NH Hamiltonian. (c) Success probability for obtaining the W-type maximally entangled state as a function of R .

state is reduced with the increase of the dissipation rate. When $R < 1$, this probability is

$$\mathcal{P} = 2 \frac{1}{1-R^2} e^{-\kappa T/2} \sin^2(\Omega T). \quad (11)$$

For $R > 1$, \mathcal{P} is

$$\mathcal{P} = 2 \frac{1}{R^2-1} e^{-\kappa T/2} \sinh^2(\Omega T). \quad (12)$$

Fig. 1d presents this probability as a function of R . The result implies that, for a given inter-qubit coupling strength, the time needed to achieve the maximal entanglement is shortened at the price of the decrease of the success probability.

THREE-QUBIT ENTANGLEMENT SPEEDUP

We note that the scheme can be directly generalized to realize dissipation-based three-qubit entanglement acceleration. The system involves two Hermitian qubits, each of which is coupled to a NH qubit with the coupling strength Ω , as shown in Fig. 2a. For the no-jump evolution trajectory, the system dynamics is governed by the NH Hamiltonian

$$\hat{\mathcal{H}}_{NH} = \lambda[\hat{\sigma}_1^+ (\hat{\sigma}_2^- + \hat{\sigma}_3^-) + H.c.] - i \frac{\kappa}{2} |1\rangle_1 \langle 1|. \quad (13)$$

In the single-excitation subspace $\{|1, 0, 0\rangle, |0, 1, 0\rangle, |0, 0, 1\rangle\}$, the system has three

eigenenergies, given by

$$\begin{aligned} E_0 &= 0, \\ E_{\pm} &= -i\kappa/4 \pm \Lambda, \end{aligned} \quad (14)$$

where $\Lambda = \sqrt{2\lambda^2 - \kappa^2/16}$. The corresponding eigenstates are

$$\begin{aligned} |\Phi_0\rangle &= \frac{1}{\sqrt{2}}(|0, 1, 0\rangle - |0, 0, 1\rangle), \\ |\Phi_j\rangle &= \mathcal{N}_{\pm}(E_{\pm}|1, 0, 0\rangle + \sqrt{2}\lambda|\phi_b\rangle), \end{aligned} \quad (15)$$

where $|\phi_b\rangle = \frac{1}{\sqrt{2}}(|0, 1, 0\rangle + |0, 0, 1\rangle)$. When the system is initially in the state $|\psi(0)\rangle = |1, 0, 0\rangle$, the state evolution associated to the no-jump trajectory is

$$|\Psi(t)\rangle = \mathcal{M}(\mathcal{C}|1, 0, 0\rangle - i\mathcal{D}|\phi_b\rangle), \quad (16)$$

where $\mathcal{M} = \sqrt{\mathcal{C}^2 + \mathcal{D}^2}$. When $R < \sqrt{2}$, the coefficients \mathcal{C} and \mathcal{D} are given by

$$\begin{aligned} \mathcal{C} &= \cos(\Lambda t) - \frac{\kappa}{4\Lambda} \sin(\Lambda t), \\ \mathcal{D} &= \frac{\lambda}{\Lambda} \sin(\Lambda t). \end{aligned} \quad (17)$$

For $R > \sqrt{2}$, the trigonometric functions are replaced by the corresponding hyperbolic functions, with $\Lambda = \sqrt{\kappa^2/16 - 2\lambda^2}$.

When $|\mathcal{C}| = |\mathcal{D}|/\sqrt{2}$, $|\Psi(t)\rangle$ corresponds to the three-qubit W-type maximally entangled state [34]

$$|\Psi_w\rangle = (e^{i\phi}|1, 0, 0\rangle + |0, 1, 0\rangle + |0, 0, 1\rangle)/\sqrt{3}. \quad (18)$$

For such a W state, any two qubits have a concurrence of $2/3$. When $R < \sqrt{2}$, the rescaled three-qubit W-state entangling time is given by

$$T_{rs} = \frac{\sqrt{2}}{\sqrt{2 - R^2} \arccos(1/\sqrt{3})} \arctan \frac{\sqrt{2 - R^2}}{1 + R}. \quad (19)$$

Here T_{rs} is defined as the ratio between the W-state generation times for the NH and Hermitian systems, $T_{rs} = T/\tau$, where $\tau = \frac{1}{\sqrt{2}\lambda} \arccos(1/\sqrt{3})$. For $R > \sqrt{2}$, the rescaled W-state entangling time is

$$T_{rs} = \frac{\sqrt{2}}{\sqrt{R^2 - 2} \operatorname{arcosh}(1/\sqrt{3})} \operatorname{arc tanh} \frac{\sqrt{R^2 - 1}}{1 + R}. \quad (20)$$

The rescaled W-state generation time T_{sc} , as a function of R , is presented in Fig. 2b, which confirms that T_{sc} is smaller than 1 when $\kappa \neq 0$, verifying the non-Hermiticity-enabled acceleration of the W state generation. The result demonstrates that the time needed to reach the W-type maximally entangled state monotonously decreases with the increase of κ for $\lambda < \kappa/4\sqrt{2}$. When $R < \sqrt{2}$, the

success probability for producing the W-type maximally entangled state is

$$\mathcal{P} = \frac{3}{2(2 - R^2)} e^{-\kappa T/2} \sin^2(\Lambda T). \quad (21)$$

For $R > \sqrt{2}$, \mathcal{P} is given by

$$\mathcal{P} = \frac{3}{2(R^2 - 2)} e^{-\kappa T/2} \sinh^2(\Lambda T). \quad (22)$$

which decreases with the increase of R , as shown in Fig. 2c.

CONCLUSION

In conclusion, we have presented a scheme for exploiting dissipation to speed up entanglement evolution for one NH qubit and one Hermitian qubit, interacting with each other via swapping a single excitation. When the excitation is initially possessed by the NH qubit, the system can conditionally evolve to a maximally entangled state within a time shorter than that needed for the Hermitian system with the same inter-qubit coupling strength. Neither does the three-level configuration nor individual driving of the qubits are required. The time needed to achieve the maximal entanglement monotonously decreases with the increase of the dissipation rate at the price of decreasing success probability. We further show that scheme can be extended to the three-qubit case, where one NH qubit initially in its excited state is coupled to two Hermitian qubits initially in their ground states. For the no-jump evolution trajectory, the time required to produce the W state is reduced by the dissipation of the NH qubit.

This work was supported by the National Natural Science Foundation of China under Grant No. 12474356.

* E-mail: linlh98@163.com

† E-mail: lipengbo@mail.xjtu.edu.cn

- [1] W. H. Zurek, Decoherence, einselection, and the quantum origins of the classical, *Rev. Mod. Phys.* 75, 715 (2003).
- [2] M. Brune *et al.*, Observing the Progressive Decoherence of the ‘‘Meter’’ in a Quantum Measurement, *Phys. Rev. Lett.* 77, 4887 (1996).
- [3] S. Deléglise *et al.*, Reconstruction of non-classical cavity field states with snapshots of their decoherence, *Nature* 455, 510 (2008).
- [4] C. J. Myatt *et al.*, Decoherence of quantum superpositions through coupling to engineered reservoirs, *Nature* 403, 269 (2000).
- [5] N. Moiseyev, *Non-Hermitian Quantum Mechanics* (Cambridge Univ. Press, 2011).

- [6] S. K. Özdemir, S. Rotter, F. Nori, and L. Yang, Parity-time symmetry and exceptional points in photonics, *Nat. Mater.* 18, 783–789 (2019).
- [7] M.-A. Miri and A. Alù, Exceptional points in optics and photonics, *Science* 363, eaar7709 (2019).
- [8] E. J. Bergholtz, J. C. Budich, and F. K. Kunst, Exceptional topology of non-Hermitian systems, *Rev. Mod. Phys.* 93, 015005 (2021).
- [9] K. Ding, C. Fang, and G. Ma, Non-Hermitian topology and exceptional-point geometries, arXiv:2204.11601.
- [10] K. Wang, L. Xiao, J. C. Budich, W. Yi, and Peng Xue, Simulating exceptional non-Hermitian metals with single-photon interferometry, *Phys. Rev. Lett.* 127, 026404 (2021).
- [11] F. E. Öztürk *et al.*, Observation of a non-Hermitian phase transition in an optical quantum gas, *Science* 372, 88 (2021).
- [12] L. Ding *et al.*, Experimental determination of PT-symmetric exceptional points in a single trapped ion, *Phys. Rev. Lett.* 126, 083604 (2021).
- [13] W.-C Wang *et al.*, Observation of PT-symmetric quantum coherence in a single-ion system, *Phys. Rev. A* 103, L020201 (2021).
- [14] P. Peng *et al.*, Anti-parity-time symmetry with flying atoms, *Nat. Phys.* 12, 1139 (2016).
- [15] J. Li *et al.*, Observation of parity-time symmetry breaking transitions in a dissipative Floquet system of ultracold atoms, *Nat. Commun.* 10, 855 (2019).
- [16] Z. Ren *et al.*, Chiral control of quantum states in non-Hermitian spin-orbit-coupled fermions, *Nature Physics* volume 18, 385 (2022).
- [17] Y. Wu *et al.*, Observation of parity-time symmetry breaking in a single-spin system, *Science* 364, 878 (2019).
- [18] W. Liu, Y. Wu, C-K. Duan, X. Rong, and J. Du, Dynamically encircling an exceptional point in a real quantum system, *Phys. Rev. Lett.* 126, 170506 (2021).
- [19] W. Zhang *et al.*, Observation of Non-Hermitian Topology with Nonunitary Dynamics of Solid-State Spins, *Phys. Rev. Lett.* 127, 090501 (2021).
- [20] M. Naghiloo, M. Abbasi, Yogesh N. Joglekar, and K. W. Murch, Quantum state tomography across the exceptional point in a single dissipative qubit, *Nat. Phys.* 15, 1232 (2019).
- [21] Z. Wang *et al.*, Observation of the exceptional point in superconducting qubit with dissipation controlled by parametric modulation, *Chin. Phys. B* 30, 100309 (2021).
- [22] Y. Choi *et al.*, Quasieigenstate coalescence in an atom-cavity quantum composite, *Phys. Rev. Lett.* 104, 153601 (2010).
- [23] T. Gao *et al.*, Observation of non-Hermitian degeneracies in a chaotic exciton-polariton billiard, *Nature* 526, 554 (2015).
- [24] J. Doppler *et al.*, Dynamically encircling an exceptional point for asymmetric mode switching, *Nature* 537, 76-79 (2016).
- [25] D. Zhang, X.-Q. Luo, Y.-P. Wang, T.-F. Li, and J. Q. You, Observation of the exceptional point in cavity magnon-polaritons, *Nature Commun.* 8, 1368 (2017).
- [26] W. Tang *et al.*, Exceptional nexus with a hybrid topological invariant, *Science* 370, 1077 (2020).
- [27] K. Wang *et al.*, Generating arbitrary topological windings of a non-Hermitian band, *Science* 371, 1240 (2021).
- [28] Y. S. S. Patil *et al.*, Measuring the knot of degeneracies and the eigenvalue braids near a third-order exceptional point, *Nature* 607, 271-275 (2022).
- [29] Q. Zhang *et al.*, Observation of Acoustic Non-Hermitian Bloch Braids and Associated Topological Phase Transitions, *Phys. Rev. Lett.* 130, 017201 (2023).
- [30] W. Tang, K. Ding, and G. Ma, Realization and topological properties of third-order exceptional lines embedded in exceptional surfaces, arXiv:2211.15921 (2022).
- [31] P.-R. Han *et al.*, Exceptional entanglement phenomena: non-Hermiticity meeting nonclassicality, *Phys. Rev. Lett.* 131, 260201 (2023).
- [32] Z.-Zhao Li, W. Chen, M. Abbasi, K. W. Murch, and K. B. Whaley, Speeding up entanglement generation by proximity to higher-order exceptional points, *Phys. Rev. Lett.* 131, 100202 (2023).
- [33] W. K. Wootters, Entanglement of formation of an arbitrary state of two qubits, *Phys. Rev. Lett.* 80, 2245 (1998).
- [34] W. Dür, G. Vidal, and J. I. Cirac, Three qubits can be entangled in two inequivalent ways, *Phys. Rev. A* 62, 062314 (2000).